

## Chapter 2

# Origin of Glass Formation

Identifying the main control parameter that dominates the slow dynamics in glass-forming liquids, giving rise to the dynamic arrest at  $T_g$ , has been a point of debate for many years. Theoretical predictions consider two extreme cases: thermally activated processes on a constant density “energy landscape” and free-volume theories [1, 2] (Chap. 1). In the former picture [3, 4], the controlling parameter is temperature ( $T$ ), the landscape is considered as fixed, and the super-Arrhenius  $\tau(T)$  is attributed to changes in the barriers and the minima encountered in the exploration of the landscape. In the latter picture, the controlling parameter is volume ( $V$ ) or better its corresponding intensive variable, the density ( $\rho$ ), and the slowing-down results from the decrease of the available or “free” volume. Clearly, these pictures should be considered as extreme cases since molecular transport, in general, is driven by thermally activated processes with potential energy barriers that depend on local density. Since changing  $T$  affects both the thermal energy ( $k_B T$ ) and the density, it is impossible to separate the two effects by  $T$  alone. In order to disentangle the effects of  $T$  and  $\rho$  on the dynamics, pressure-dependent measurements have been of paramount importance since pressure ( $P$ ) can be applied isothermally (affecting only  $\rho$ ) and have been employed to provide a quantitative assessment of their relative importance.

In this chapter, we provide two approaches that lead to a better understanding of the dynamics in the vicinity of the glass transition. The first one is based on the newly observed feature of dynamics in this class of materials, which is known as “thermodynamic scaling.” The second approach emphasizes the role of molecular volume and local packing on glass transition dynamics.

## 2.1 Thermodynamic Scaling of Molecular Dynamics in Viscous Systems

### 2.1.1 A General Idea of Thermodynamic Scaling

The first interesting results in the area of thermodynamic scaling have been obtained for a typical van der Waals (vdW) liquid. Analyzing inelastic neutron

scattering data from ortho-terphenyl (OTP), Tölle [5] observed that the use of the well-known Lennard-Jones (LJ) potential, with its repulsive and attractive parts proportional to the following powers of interspecies distance  $r$ ,  $r^{-12}$ , and  $r^{-6}$ , respectively, seems to be sufficient to describe molecular dynamics of vdW liquid. This assumption enabled him to express the relaxation times in terms of  $T^{-1}V^{-4}$ . This has been successfully applied by Dreyfus et al. [6] to plot rotational relaxation times for different isotherms, obtained from light-scattering data of OTP, onto a single master curve. The promising result has initiated intensive investigations of its application in other glass-forming liquids. It has been quickly pointed out by a few research teams [7–10] that the thermodynamic scaling found in OTP is generally not valid for other glass formers that belong to different kinds of materials such as vdW liquids (e.g., BMMPC, BMPC, salol, PDE, and PC), polymers (e.g., 1,2-PB, 1,4-PB, PVME, PMMA, and PVAc), and hydrogen bonded systems (e.g., sorbitol). Therefore, a generalized variable  $\Gamma$  has been proposed, which could replace  $T$ . Consequently, a relaxation time  $\tau$  (or equivalent viscosity  $\eta$ , excluding materials revealing the decoupling phenomenon described in [11], which suggests a different scaling exponent  $\gamma$  for the relaxation time and viscosity) has been expressed as some scaling function  $J$  of the variable  $\Gamma$  [9]:

$$\log_{10}(\tau) = J(\Gamma), \quad (2.1)$$

where  $\Gamma = T^{-1}V^{-\gamma}$  or  $\Gamma = \rho^\gamma/T$ .

Such an approach has brought a noticeable success (see Fig. 2.1). These and other related efforts enabled extracting a single material-dependent scaling exponent  $\gamma$  for

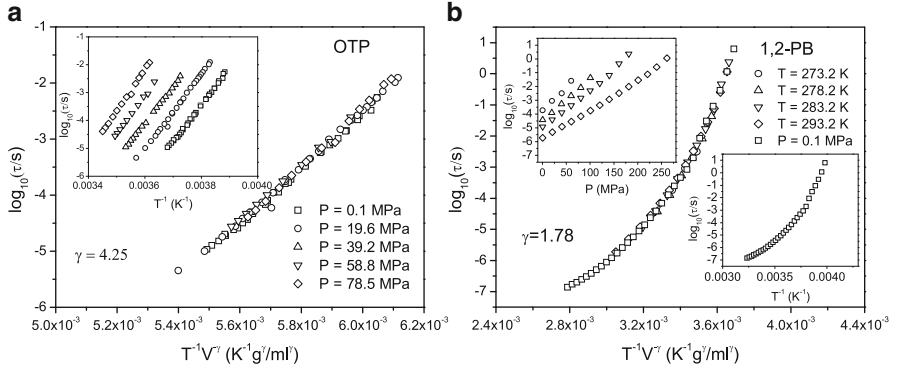


**Fig. 2.1** Examples of the temperature dependences of dielectric relaxation times vs. the scaling quantity  $\Gamma = T^{-1}V^{-\gamma}$  for (a) a typical van der Waals liquid: ortho-terphenyl (OTP), and (b) a polymer 1,2-polybutadiene (1,2-PB) with molecular mass equal to 3000 g/mol. The value of the scaling exponent  $\gamma = 4.25$  established [8] for dielectric relaxation data obtained in various isobaric conditions for OTP differs slightly from the value  $\gamma = 4.0$  found on the basis of other measurement methods [6, 8]. The obtained value  $\gamma = 1.78$  for 1,2-PB is slightly smaller than the value  $\gamma = 1.9$  reported in [7], where a smaller data set (excluding two isotherms at  $T = 273.2$  K and  $278.2$  K) than that used here has been used

many glass formers, which allowed the superposition of different isothermal and isobaric relaxation times into a single master curve in accordance with (2.1). The values of the parameter  $\gamma$  obtained for several dozen materials are presented in Table 1.1 (see Appendix 1).

The scaling quantity  $\Gamma$  can be deduced from the generalized Lennard-Jones potential [12]

$$U_{\text{LJ}}(r_{ij}) = 4\epsilon_{ij} \left[ \left( \frac{\sigma_{ij}}{r_{ij}} \right)^{m_r} - \left( \frac{\sigma_{ij}}{r_{ij}} \right)^{n_a} \right], \quad (2.2)$$

where  $r$  is a distance between species  $i$  and  $j$ , and  $\epsilon_{ij}$  and  $\sigma_{ij}$  are parameters expressed in energy and distance units, respectively, and dependent on interacting particular species. The first and second terms on the right-hand side of (2.2) correspond to the repulsive and attractive interactions between the species. If we need to keep the same proportion between the exponents  $m_r$  and  $n_a$ , as is in the original formula of the Lennard-Jones potential, then the generalization taking into account the scaling exponent  $\gamma$  results to  $m_r = 3\gamma$  and  $n_a = 3\gamma/2$ . However, many authors [13–16] are inclined to regard only the repulsive part of the generalized Lennard-Jones potential (Fig. 2.2) as mainly responsible for the thermodynamic scaling property. Therefore, the assumption  $m_r = 3\gamma$  is usually treated as sufficient to explain the scaling property, while the exponent  $n_a$  is left unlimited in that sense. It is worth noting that in relation to the modified LJ potential, the scaling exponent  $\gamma$  can be interpreted as an indicator of “softness” of the intermolecular repulsive potential. A straightforward explanation of the form of scaling quantity,  $\Gamma = T^{-1}V^{-\gamma}$ , can be reduced by noting that the repulsive term (2.2) of the generalized

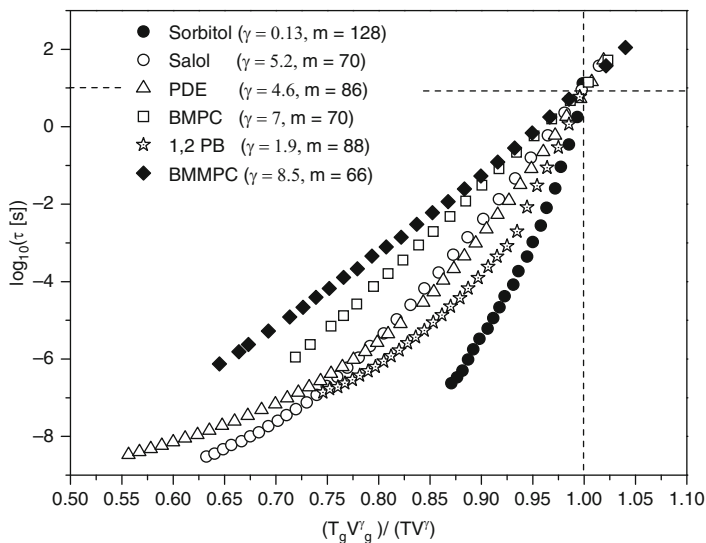


**Fig. 2.2** A modified Angell plot of the rescaled fragility (similar to Fig. 4 from [7])

LJ potential can be written in the form proportional to  $r^{-3\gamma}$  and substituting simply  $V \sim r^3$  to the relationship  $V^{-\gamma} \sim r^{-3\gamma}$ . A somewhat more sophisticated account for the form of the quantity  $\Gamma$  will be presented at the end of this chapter by using the Euler theorem on homogeneous functions.

### 2.1.2 A New Measure of the Relative Temperature–Volume Influence on Molecular Dynamics

The form of the scaling quantity  $\Gamma$  suggests that the parameter  $\gamma$  reflects the relative thermal and volume effect on molecular dynamics. Thus, when  $\gamma$  decreases to zero,  $\Gamma$  tends to rely more on  $T$ , implying that the intermolecular free volume contribution will decrease and the influence of thermal activation will increase. This observation naturally encourages to search for relations of the scaling exponent  $\gamma$  with quantities used earlier for evaluating the relative influence of the thermal activation and free volume on relaxation phenomena near the glass transition. As shown in Chap. 1, the quantities commonly employed to achieve this aim are the dynamic ratio  $Q_V/Q_P$ , i.e., the ratio of the isochoric activation energy over the activation enthalpy [17, 18], and  $\alpha_P/|\alpha_T|$ , the ratio of the isobaric and isochoric thermal volume expansivities [19], calculated at the glass temperature  $T_g$ . To express the ratio of energies (1.32) by means of the scaling exponent  $\gamma$ , we first show how the fragility parameter  $m$  can be redefined by using the scaling quantity  $\Gamma$  [7, 20]. As can be seen in Fig. 2.2, if we replace the ratio  $T_g/T$  by the scaled ratio  $\Gamma/\Gamma_g$ , where  $\Gamma_g = T_g^{-1}V_g^{-\gamma}$  is a value of the scaling quantity  $\Gamma$  at the glass transition temperature, we can prepare a modified Angell plot analogous to that shown in Chap. 1 (see Fig. 1.17), and consequently introduce a rescaled definition of the fragility parameter. In general, the definition can be formulated as follows:

$$m = \left( \frac{d \log_{10}(\tau)}{d(\Gamma/\Gamma_g)} \right) \Big|_{\Gamma=\Gamma_g}. \quad (2.3)$$

More precisely, considering isobaric and isochoric conditions (on which the fragility parameter is usually determined), one can propose the rescaled definitions of the isobaric and isochoric fragilities:

$$m_P = \left( \frac{d \log_{10}(\tau)}{d(\Gamma/\Gamma_g)} \right)_P \Big|_{\Gamma=\Gamma_g}, \quad (2.4)$$

$$m_V = \left( \frac{d \log_{10}(\tau)}{d(\Gamma/\Gamma_g)} \right)_V \Big|_{\Gamma=\Gamma_g}. \quad (2.5)$$

Using the standard definitions of the isobaric and isochoric fragilities (see Chap. 1), one can show [21–23] that these quantities are interrelated,

$$\begin{aligned}
 m_P &= \left. \frac{\partial \log_{10}(\tau)}{\partial(T_g/T)} \right|_{P=\text{const}, T=T_g} \\
 &= \left. \frac{\partial \log_{10}(\tau)}{\partial(T_g/T)} \right|_{V=\text{const}, T=T_g} + \left. \frac{\partial \log_{10}(\tau)}{\partial V} \right|_{T=\text{const}, T=T_g} \left. \frac{\partial V}{\partial(T_g/T)} \right|_{P=\text{const}, T=T_g} \\
 &= \left. \frac{\partial \log_{10}(\tau)}{\partial(T_g/T)} \right|_{V=\text{const}, T=T_g} \\
 &\quad - \left( \left. \frac{\partial \log_{10}(\tau)}{\partial(T_g/T)} \right|_{V=\text{const}, T=T_g} \bigg/ \left. \frac{\partial V}{\partial(T_g/T)} \right|_{\tau=\text{const}, T=T_g} \right) \left. \frac{\partial V}{\partial(T_g/T)} \right|_{P=\text{const}, T=T_g}.
 \end{aligned} \tag{2.6}$$

The last conversion in (2.6) results from the rule of the implicit partial derivative. Taking into account the standard definition of the isochoric fragility,  $m_V$ , as well as the definitions of the isobaric and isochronic thermal volume expansivities,  $\alpha_P$  and  $\alpha_\tau$ , one can derive the following relationship between the fragilities  $m_P$  and  $m_V$ :

$$m_P = m_V \left( 1 - \frac{\alpha_P}{\alpha_\tau} \right), \tag{2.7}$$

where the fragilities and the expansivities should be calculated as the limit values taken from the side of the supercooled region at the point  $(P_\tau, V_\tau, T_\tau)$  determined by the same relaxation time  $\tau$  which is usually chosen to define the glass transition. As a result, the relations given by (2.7) and (1.32) allow us to express the ratio of activation energies by the ratio of fragilities as follows:

$$\left. \frac{Q_V}{Q_P} \right|_{T=T_g} = \frac{m_V}{m_P}. \tag{2.8}$$

This last equation also follows directly from the ratio of  $m_V (= (1/T_g)(\partial \log_{10}(\tau)/\partial(1/T))_V)$  with  $m_P (= (1/T_g)(\partial \log_{10}(\tau)/\partial(1/T))_P)$  calculated at  $T = T_g$ . In this way, we gain not only a new expression for the measure of the relative effect of  $T$  and  $V$  on molecular dynamics near the glass temperature, but also an additional insight into values reached by this measure. If the quantity  $m_V/m_P$  approaches 1, i.e., if the fragility  $m_V$ , evaluated at constant volume, and the fragility  $m_P$ , obtained at constant pressure, both determined at the same glass transition temperature  $T_g$ , are equal, then one can state that thermal activation plays a decisive role in the dynamic behavior. On the contrary, the dynamics is mainly governed by an intermolecular free volume if the ratio  $m_V/m_P$  approaches 0, due to the isochoric fragility decreasing toward zero.

Analogous calculations can be made in terms of the scaling quantity  $\Gamma$ , by replacing  $T_g/T$  by  $\Gamma/\Gamma_g$ . As the ratio of partial derivatives of the scaling quantity  $\Gamma$  yields

$$\begin{aligned} \left( \frac{\partial V}{\partial(\Gamma/\Gamma_g)} \right)_P \Big|_{\Gamma=\Gamma_g} / \left( \frac{\partial V}{\partial(\Gamma/\Gamma_g)} \right)_\tau \Big|_{\Gamma=\Gamma_g} &= \left( \frac{\partial \Gamma}{\partial V} \right)_\tau \Big|_{\Gamma=\Gamma_g} / \left( \frac{\partial \Gamma}{\partial V} \right)_P \Big|_{\Gamma=\Gamma_g} \\ &= \frac{\left( \frac{\partial \Gamma}{\partial V} \right)_\tau \Big|_{\Gamma=\Gamma_g}}{\left( \frac{\partial \Gamma}{\partial T} \right)_V \Big|_{\Gamma=\Gamma_g} \left( \frac{\partial T}{\partial V} \right)_P \Big|_{\Gamma=\Gamma_g}} = \frac{\gamma T V^{-1}}{\left( \frac{\partial T}{\partial V} \right)_P \Big|_{\Gamma=\Gamma_g}} = \gamma T_g \alpha_P(T_g), \end{aligned} \quad (2.9)$$

the relation between rescaled isobaric and isochoric fragilities can be formulated as follows [20, 24]:

$$m_P = m_V (1 + \gamma T_g \alpha_P(T_g)). \quad (2.10)$$

As a consequence, the scaling exponent  $\gamma$  relates to the commonly used measure of the relative contribution of thermal activation and free volume to molecular dynamics of supercooled liquids through [7, 24]

$$\frac{Q_V}{Q_P} \Big|_{T=T_g} = \frac{1}{1 + \gamma T_g \alpha_P(T_g)}. \quad (2.11)$$

Taking into account the empirical rule [25, 26]  $\alpha_P T_g \approx \text{const}$  at ambient pressure, the scaling exponent  $\gamma$  can be considered as a new measure of the relative degree to which temperature and density control the dynamics [7, 27]. On the basis of (2.11), two extreme cases can be predicted. If  $\gamma = 0$ , then thermal energy should fully dominate molecular dynamics. If  $\gamma$  tends to infinity – that corresponds to the limiting case of a hard sphere potential, an intermolecular free volume should decide on the dynamics.

Moreover, the expected correlation between the exponent  $\gamma$  and the ratio  $Q_V/Q_P$ , has been suggested by Casalini and Roland [7, 27] (see Fig. 2.3). According to the correlation and after an analysis of values of the exponent  $\gamma$  for various materials (e.g., see Table 1.1 in Appendix 1), one can note some regularity. The smallest values of the scaling exponent are established for some hydrogen-bonded systems where the thermodynamic scaling is accepted to be valid. As  $\gamma$  increases, we first find the characteristic scaling exponents for polymers, and then evaluate the largest values of  $\gamma$  mainly for vdW liquids.

The use of the scaling exponent  $\gamma$  as the intermolecular potential-dependent measure of the relative influence of temperature/density on the molecular dynamics can be additionally substantiated by considering the approach presented by Alba-Simionesco

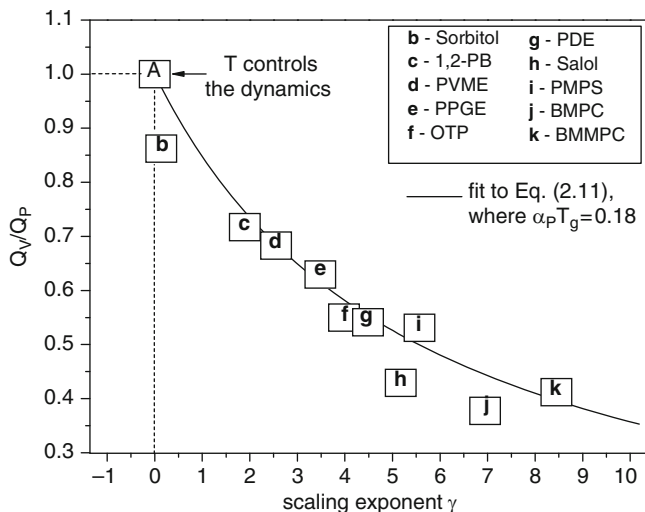


**Fig. 2.3** Demonstration of the use of the scaling exponent  $\gamma$  for evaluating the relative effect of temperature and volume on molecular dynamics (data taken from Fig. 3 in [7])

and coworkers [23]. Normally, the thermodynamic scaling can be valid due to a closely related effect of density scaling of energy barriers for different dynamic processes in supercooled liquids. In their approach, they assume and show [23], by using results obtained from measurements on the organic glass-former OTP and the polymer polyvinyl methyl ether (PVME) as well as from computer simulations performed for a binary LJ liquid model, that the activation energy that depends on temperature and density,  $E(T, \rho)$ , can be scaled satisfactorily with density by means of some general equation:

$$\frac{E(T, \rho)}{e(\rho)} = J_E \left[ \frac{T}{e(\rho)} \right], \quad (2.12)$$

where functions  $J_E$  and  $e(\rho)$  are system dependent, and the energy barrier  $E(T, \rho)$  is defined by the following expression for the relaxation time

$$\tau(T, \rho) = \tau_\infty(\rho) \exp \left[ \frac{E(T, \rho)}{T} \right]. \quad (2.13)$$

The energy scaling described by (2.12) leads to the collapse of the data onto a single master curve,  $E(T, \rho)/e(\rho)$  vs.  $T/e(\rho)$ , if the function  $e(\rho)$ , interpreted as the activation barrier in the high temperature limit,  $E_\infty(\rho)$ , is assumed to be proportional to  $\rho^\gamma$ , where  $\gamma$  is the same scaling exponent as that used in (2.1). Consequently, one can formulate a scaling equation for the relaxation time  $\tau$  (or the viscosity  $\eta$ ),

$$\log_{10}[\tau(T, \rho)] = J_\rho(X) \quad (2.14)$$

where  $X = e(\rho)/T$ . It can be easily seen that the scaling equations (2.1) and (2.14) are equivalent and the scaling quantities are proportional to each other, i.e.,  $\Gamma \propto X$ .

In accordance with the idea of thermodynamic scaling, both  $\Gamma$  and  $X$ , independent of the thermodynamic conditions, assume a constant value at a given relaxation time  $\tau$ . This important feature results in some obvious equations:

$$\left(\frac{\partial \Gamma}{\partial T}\right)\bigg|_{\tau=\text{const}} = 0 \quad \text{and} \quad \left(\frac{\partial X}{\partial T}\right)\bigg|_{\tau=\text{const}} = 0. \quad (2.15)$$

After simple calculations based on the above equations, namely,

$$1 + \left(\gamma TV^{-1} \frac{\partial V}{\partial T}\right)\bigg|_{\tau=\text{const}} = 0 \quad \text{and} \quad 1 + \left(T \frac{\partial \ln(e(\rho))}{\partial \ln(\rho)} \frac{\partial \ln(\rho)}{\partial T}\right)\bigg|_{\tau=\text{const}} = 0, \quad (2.16)$$

we can derive two closely connected relations:

$$\gamma T_\tau \alpha_\tau = -1 \quad \text{and} \quad \frac{\partial \ln(e(\rho))}{\partial \ln(\rho)} T_\tau \alpha_\tau = -1, \quad (2.17)$$

where  $T_\tau$  is the temperature at which the structural relaxation time  $\tau$  is equal to the value that is usually chosen to equate the glass transition temperature  $T_g$  with  $T_\tau$ . Of course, the relations presented in (2.17) are identical if it is assumed that  $e(\rho) = \rho^\gamma$ . An interpretative advantage of the approach based on the density scaling of the energy barrier can be seen when we refer to the ratio of the isobaric and isochronal thermal volume expansivities,  $\alpha_P/\alpha_\tau$ , that determine the relationship shown in (2.7) and its scaled representation (2.10). According to (2.17), the dependence  $m_P$  on  $m_V$  can be reformulated as follows:

$$m_P = m_V \left(1 + \alpha_P T_g \frac{\partial \ln(e(\rho))}{\partial \ln(\rho)}\right). \quad (2.18)$$

In addition, let us notice that the product  $\alpha_P T_g = -(\partial \ln(\rho)/\partial \ln(T))_P|_{T=T_g}$ . This suggests that one can extract from the ratio  $\alpha_P/\alpha_\tau$  the contributions of both effects: the temperature dependence of a system density measured by the product  $\alpha_P T_g$ , and the density dependence of relaxation times quantified by the derivative  $\partial \ln(e(\rho))/\partial \ln(\rho)$ . This again shows that the ratio  $\alpha_P/\alpha_\tau$  is a measure of the relative influence of temperature and density on molecular dynamics of the investigated system. Moreover, in the context of the previous considerations, the scaling exponent  $\gamma$  can be treated as a system-specific parameter that characterizes the density dependence of relaxation times.

It is worth noting that the condition of the constancy of  $\Gamma$  at a given relaxation time,  $T_\tau^{-1} V_\tau^{-\gamma} = \text{const}$ , which underlies (2.15), enables finding [28] a convenient method for determining the scaling exponent  $\gamma$ . At the glass temperature, a linear logarithmic dependence  $T_g(V_g)$  is found,



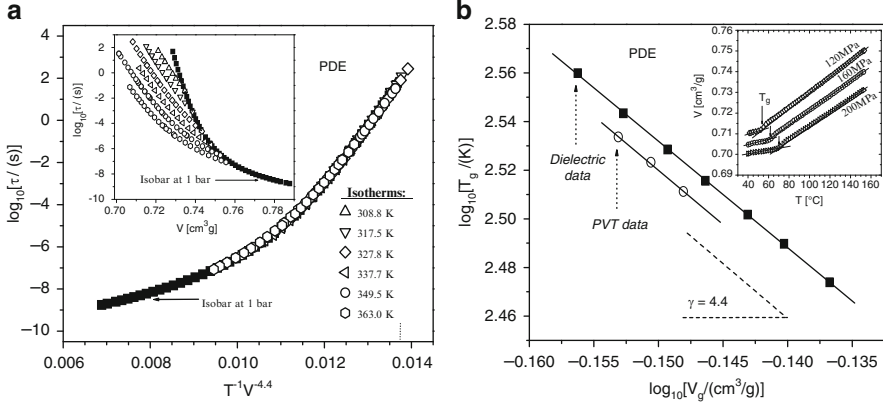


**Fig. 2.4** (a) Thermodynamic scaling vs. the quantity  $\Gamma = T^{-1}V^{-\gamma}$ . The *inset* shows the isotherms and the isobar at atmospheric pressure as a function of volume; (b) Logarithmic plot of the glass transition temperature  $T_g$  vs. the glass transition volume  $V_g$  for PDE. *Closed squares* indicate data from dielectric measurements. *Open circles* represent data from *PVT* measurements. *Solid lines* are respective fits to the dielectric and *PVT* data according to (2.19) with the same slope  $\gamma$ . The *inset* shows the specific volume vs. temperature data at different isobars obtained from *PVT* measurements near the glass transition temperature, which have been used to determine  $T_g$  from *PVT* data

$$\log_{10} T_g = A - \gamma \log_{10} V_g \quad (2.19)$$

with parameters  $A$  and scaling exponent  $\gamma$ , that can be obtained by a simple linear regression.

As an example for PDE, we present how this procedure works (Fig. 2.4b) in comparison with the standard way of determining the scaling exponent  $\gamma$  from the plot (Fig. 2.4a) according to (2.1). From the  $T_g(V_g)$  representation (2.19), we find, both from dielectric and *PVT* data,  $\gamma = 4.4$ , which corresponds nicely with the same parameter obtained from the standard procedure of the thermodynamic scaling. This procedure, following from (2.19), emphasizes that the scaling exponent  $\gamma$  can be obtained from *PVT* measurements alone [28] (although in general evaluation of the glass transition point ( $T_g, V_g$ ) using the *PVT* data can be insufficiently accurate). It further suggests that the dynamic and thermodynamic properties are expected to be strongly correlated.

### 2.1.3 The Relaxation Time Description in Accordance with Thermodynamic Scaling

After the general considerations about thermodynamic scaling, it is worth mentioning some attempts to determine explicit expressions for the scaling functions  $J$  and  $J_\rho$  implicitly introduced into (2.1) and (2.14). Casalini and Roland have proposed

several scaled equations for the relaxation time. At first, they have indicated [7] that a simple expression,

$$\log_{10}[\tau(\Gamma)] = \log_{10}(\tau_{\infty}) + C\Gamma, \quad \Gamma = T^{-1}V^{-\gamma}, \quad (2.20)$$

which assumes a volume-dependent activation energy,  $C/V^{\gamma}$ , where  $C$  is a constant and  $\gamma$  is the scaling exponent, can rationalize the dependence of the ratio  $Q_V/Q_P$  on the exponent  $\gamma$  depicted in Fig. 2.3. However, as the same authors noticed, (2.20) cannot correctly describe any experimental dependence of relaxation times on the scaling quantity  $\Gamma$ , because each of them reveals a nonlinear behavior. Searching for some phenomenological description of the dependence  $\log_{10}[\tau(\Gamma)]$ , they rejected the VFT equation due to its intrinsic singularity at temperature  $T_0$  and in the next step, they applied [20] the modified Cohen–Grest equation

$$\log_{10}[\tau(\Gamma)] = \log_{10}(\tau_{\infty}) + \frac{A}{\Gamma^{-1} - \Gamma_0^{-1} + \left[ (\Gamma^{-1} - \Gamma_0^{-1})^2 + B\Gamma^{-1} \right]}, \quad (2.21)$$

$$\Gamma = T^{-1}V^{-\gamma},$$

where  $A$ ,  $B$ , and  $\Gamma_0$  are constants. However, the validity of the Cohen–Grest model at high pressures will be questioned [29] (see Chap. 3); therefore, it has not been further developed within the framework of thermodynamic scaling [30].

Some general scaling equation for the relaxation time has been proposed by Dreyfus et al. [8]. As mentioned earlier, these authors developed the concept of the temperature–density dependent activation barrier  $E(T, \rho)$  and its high-temperature limit  $e(\rho)$ , presented herein in (2.13) and (2.14), respectively. They suggested that  $\log_{10}[\tau(X)] = \log_{10}(\tau_{\infty}) + X\Phi(X)$ , where  $X = e(\rho)/T$ , and assumed that the equation in the high-temperature limit should obey the Arrhenius law. Consequently, it implies that  $\Phi(X)$  should tend to 1 when  $X$  approaches zero, i.e., the function  $\Phi$  should be a positive monotonously increasing function of  $1/T$  for  $T/T_g \gg \Phi(X)$ , if we recall the Angell plot construction. As for the function  $\Phi$ , it has been chosen as  $\exp(bX)$ , which met such requirements if  $b$  is a material-dependent positive constant. Then, formulating the scaling equation in terms of the scaled quantity  $X/X_g$ , reduced with respect to the glass transition point at which the relaxation time  $\tau_g = \tau(\rho_g, T_g)$ , one can derive the following general expression [8]:

$$\log_{10}[\tau(X)] = \log_{10}(\tau_{\infty}) + \log_{10}\left(\frac{\tau_g}{\tau_{\infty}}\right) \frac{X}{X_g} \exp\left[bX_g\left(\frac{X}{X_g} - 1\right)\right] \quad (2.22)$$

where typically assuming that  $e(\rho) \sim \rho^{\gamma}$  one can substitute  $X/X_g = T_g\rho^{\gamma}(T)T^{-1}\rho_g^{-\gamma}(T)$ .

Some interesting results have been achieved [13, 30] by exploiting the Avramov model (see Chap. 3) to find the scaled equation for the relaxation time:

$$\log_{10}[\tau(\Gamma_G)] = \log_{10}(\tau_\infty) + \epsilon \log_{10}(e) \left( \frac{\Gamma_G}{\Gamma_{Gr}} \right)^D, \quad \Gamma_G = T^{-1} V^{-\gamma_G}, \quad (2.23)$$

$$\Gamma_{Gr} = T_r^{-1} V_r^{-\gamma_G}$$

which can be easily reduced to its form depending on the four parameters  $\tau_\infty$ ,  $A$ ,  $D$ , and  $\gamma_G$ ,

$$\log_{10}[\tau(\Gamma_G)] = \log_{10}(\tau_\infty) + (A \Gamma_G)^D, \quad \Gamma_G = T^{-1} V^{-\gamma_G}, \quad (2.24)$$

$$A = [\epsilon \log_{10}(e)]^{\frac{1}{D}} / \Gamma_{Gr}$$

where the parameter  $\epsilon = E_{\max}/\sigma_r$  is expressed by the dispersion of the system at some reference state,  $\sigma_r$ , and the upper limit of the distribution of the energy barrier height,  $E_{\max}$ . The above equation can be derived by using the basic Avramov equation [see Chap. 3, (3.23)] converted from the viscosity  $\eta$  into the relaxation time  $\tau$ , where the system entropy,  $S$ , can be easily related to some other thermodynamic properties of the system and can be calculated from volumetric data, given at least one of the values of isobaric or isochoric heat capacity. Starting from a volume–temperature dependence of the entropy  $S(T, V)$ , unlike the original Avramov approach based on a pressure–temperature effect on entropy, one can show that

$$S(T, V) = S_r + C_V \left[ \ln\left(\frac{T}{T_r}\right) + \frac{(C_P/C_V) - 1}{T\alpha_P} \ln\left(\frac{V}{V_r}\right) \right] \quad (2.25)$$

where  $S_r$ ,  $T_r$ , and  $V_r$  denote thermodynamic variables in sequence  $S$ ,  $T$ , and  $V$  at an arbitrary chosen reference state, and  $\alpha_P$  is the isobaric thermal volume expansivity, whereas  $C_P$  and  $C_V$  are heat capacities determined at a constant pressure and a constant volume, respectively. Defining a new parameter

$$\gamma_G = \frac{(C_P/C_V) - 1}{T\alpha_P} \quad (2.26)$$

the entropy of the system can be formulated as follows:

$$S(T, V) = S_r + C_V \ln\left(\frac{TV^{\gamma_G}}{T_r V_r^{\gamma_G}}\right). \quad (2.27)$$

Introducing the above entropy formula into the basic Avramov equation (3.23), where the viscosity  $\eta$  is substituted by the relaxation time  $\tau$ , and the parameter  $\epsilon$  is usually expressed by  $\ln(\tau_g/\tau_\infty)$ , in which  $\tau_g$  is the relaxation time at the glass transition and  $\tau_\infty$  is the relaxation time in the high temperature limit, one can obtain the scaled equation for the relaxation time presented in (2.23) where its parameter  $D$  can be expressed by means of the isochoric heat capacity  $C_V$ ,

$$D = \frac{2C_V}{ZR}. \quad (2.28)$$

Here,  $R$  is the gas constant and  $Z$  is the parameter representing the degree of the system degeneracy within the Avramov model. The physical meaning of the latter is the number of available pathways for local motions per molecule or polymer segment; hence it can be roughly approximated by the coordination number of the liquid lattice.

Tests performed by Casalini et al. [13, 30] for various glass formers with the scaled model given by (2.24), where the scaled quantity  $\Gamma_{Gr}$  at a reference state was assumed to concern the glass transition point, show that the equation successfully describes experimental relaxation data. Moreover, the advantage of the application of the Avramov model to the scaled dependences of relaxation times (2.1) is its close connection with thermodynamic properties of the investigated systems. It is worth noticing that (2.25) is a consequence of several thermodynamic relationships.

As mentioned earlier, we first exploit the entropy differential,

$$dS(T, V) = \left( \frac{\partial S}{\partial T} \right)_V dT + \left( \frac{\partial S}{\partial V} \right)_T dV \quad (2.29)$$

where

$$\left( \frac{\partial S}{\partial T} \right)_V = \left( \frac{\partial S}{\partial U} \right)_V \left( \frac{\partial U}{\partial T} \right)_V = \frac{1}{T} C_V \quad (2.30)$$

on the basis of the definitions of the isochoric heat capacity and the internal energy  $U$ .

To find an appropriate form for the isothermal change of entropy, we consider some thermodynamic quantities and transformations. Using the Helmholtz free energy,  $F = U - TS$ , and its total differential,  $dF(T, V) = -SdT - PdV$ , it is easily seen that

$$\left( \frac{\partial S}{\partial V} \right)_T = \left( \frac{\partial P}{\partial T} \right)_V. \quad (2.31)$$

Employing the basic thermodynamic relation for the heat capacities,

$$C_P - C_V = T \left( \frac{\partial V}{\partial T} \right)_P \left( \frac{\partial P}{\partial T} \right)_V \quad (2.32)$$

allows to develop (2.31) to the formula below:

$$\left( \frac{\partial S}{\partial V} \right)_T = \left( \frac{\partial P}{\partial T} \right)_V = \frac{C_P - C_V}{TV\alpha_P}. \quad (2.33)$$

Taking into account (2.26) and (2.33) as well as using the definition of the isothermal volume compressibility,

$$\kappa_T \equiv -\frac{1}{V} \left( \frac{\partial V}{\partial P} \right)_T = \frac{1}{V} \left( \frac{\partial V}{\partial T} \right)_P \left( \frac{\partial T}{\partial P} \right)_V = \alpha_P \left( \frac{\partial T}{\partial P} \right)_V \quad (2.34)$$

where the rule of the implicit partial derivative is exploited, one can easily find that the scaling exponent  $\gamma_G$  derived in terms of the modified Avramov model can take the following form:

$$\gamma_G = \frac{V\alpha_P}{C_V\kappa_T} \quad (2.35)$$

which is the thermodynamic definition [31, 32] of a parameter called the Grüneisen constant. Casalini et al. [13] argued, by experimental testing of (2.35), that the volume dependence of  $\gamma_G$  is negligible and one can determine the Grüneisen constant from  $PVT$  data at the reference state such as the glass transition point. Thus, it can be used to represent the scaling exponent  $\gamma$  which is expected to be constant. It is worth noting that the Grüneisen constant [33] was originally defined as the isothermal change of frequency  $\nu$  in systems of quantum oscillators with system volume  $V$ ,

$$\gamma_G \equiv - \left( \frac{d \ln \nu}{d \ln V} \right)_T = - \left( \frac{r d\nu}{3\nu dr} \right)_T. \quad (2.36)$$

Keeping in mind possible limitations of using this parameter for finding the scaling exponent  $\gamma$ , such as the temperature dependence of the quantity given by (2.36) and the unknown dependence of relaxation dynamics on vibrations, we note that the Grüneisen constant can lead to some interesting conclusions. Assuming that the intermolecular potential (2.2) can be reduced to its repulsive part with the exponent  $m_r = 3\gamma$ , and further considering a lattice of phonons with the harmonic force constant for their vibrations given by  $\partial^2 U_{LJ}^r / \partial r^2 \propto v^2$ , one can prove [34] that

$$\gamma_G = \frac{1}{2}\gamma + \frac{1}{3} \quad (2.37)$$

i.e., a simple relation between the Grüneisen constant, which can be established from  $PVT$  measurements data on the basis of (2.35), and the scaling exponent  $\gamma$  used in (2.1), however, under the assumption that the exponent  $\gamma$  can be straightforwardly related to the exponent  $m_r$  in (2.2), i.e., if  $\gamma = m_r/3$ . Nevertheless, this finding clearly shows that the thermodynamic scaling can be considered as a linkage of dynamic and thermodynamic properties. Although attempts of experimental verifications of the relation given by (2.37) are frequently unsuccessful [32], its meaning does not depreciate, because the discrepancies with experimental

data can be caused by factors such as vibrations and secondary relaxations that do not contribute to the structural relaxation (or the segmental relaxation in the case of polymers), but may contribute to the thermodynamic parameters of (2.35) such as the isochoric heat capacity and the isobaric thermal volume expansivity [35]. Indeed, the Grüneisen constants calculated from (2.35) at temperatures near the glass transition temperature by using, instead of the total heat capacity,  $C_V^{\text{liq}}$ , found in the liquid phase, this value diminished by the corresponding heat capacity,  $C_V^{\text{cryst}}$ , for the crystalline state, results in values of  $\gamma_G$  that are in better agreement with the expectations [30].

In the above context, the scaled Avramov model leading to (2.23) not only yields a good description for experimental data, but also its scaling parameter,  $\gamma_G$ , suggests how the relaxation dynamics can be scaled by means of the thermodynamic properties. The advantage of the model can be related to its entropic nature. Additionally, Casalini et al. [30] showed that (2.23) can also be derived within the framework of Landau–Lifshitz thermodynamic fluctuation theory that generally concerns relaxation times governed by the entropy. The Adam–Gibbs model, the most popular among the entropic approaches, has been suggested by Alba-Simionesco and Tarjus [23] to apply in order to describe the relaxation times in terms of thermodynamic scaling,

$$\log_{10}[\tau(T, \rho)] = \log_{10}(\tau_\infty) + \frac{A(\rho)\log_{10}(e)}{TS_c(\rho, T)}, \quad (2.38)$$

where the configurational entropy,  $S_c(\rho, T) = S_c(X)$ , is a function of the same scaling quantity,  $X = e(\rho)/T$ , as in (2.14). However, Casalini et al. [30] draw our attention to the fact that the Adam–Gibbs model is characterized by some divergence of relaxation times analogous to the VFT equation, unlike the Avramov approach.

### 2.1.4 Thermodynamic Scaling on Isothermal Conditions and Its Consequences

An important and useful observation is the finding of the scaling behavior similar to that described by (2.1), but established for isothermal  $\alpha$ -relaxation times plotted vs. the inverse specific volume scaled by the specific volume at the glass transition,  $V_g/V$ . The latter can be equivalently replaced by the corresponding ratio of densities,  $\rho/\rho_g$ . It has been shown [28] that the quantity  $V_g/V$  can scale the isothermal relaxation times obtained at different temperatures onto one master curve, specific to each system both in the case of vdW liquids and polymers (see examples in Fig. 2.5a, b, respectively), that is, analogously to the scaling quantity  $\Gamma$ .

Let us see why the scaling vs.  $V_g/V$  is valid simultaneously with scaling vs.  $\Gamma$ . In order to do that, we rewrite the quantity  $\Gamma$  in the following form:

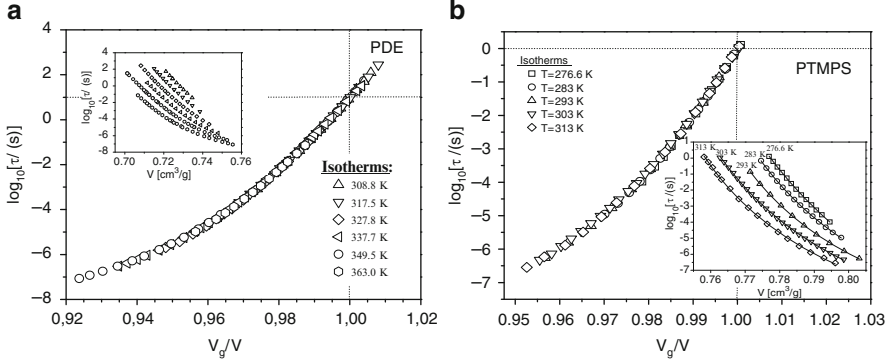


**Fig. 2.5** Scaling of isothermal structural relaxation times vs.  $V_g/V$  for representatives of (a) van der Waals liquids (PDE) and (b) polymers (PTMPS). The insets show used isotherms as functions of volume

$$T^{-1}V^{-\gamma} = \left(\frac{V_g}{V}\right)^{\gamma} T^{-1}V_g^{-\gamma}. \quad (2.39)$$

If scaling vs. the quantity  $T$  is satisfied, then the scaling exponent  $\gamma$  is constant and at the glass transition temperature,  $T_g$ , one can formulate the condition

$$T_g^{-1}V_g^{-\gamma} = \text{const.} \quad (2.40)$$

From the above simple relations expressed in (2.39) and (2.40), it can be concluded that the ratio  $V_g/V$  itself leads to the scaling of isothermal relaxation times.

It is worth emphasizing that the volume scaling leads to some important consequence concerning the isothermal fragility  $m_T$ , which implies also properties of the isochoric and isobaric steepness indices,  $m_V$  and  $m_P$ . If the scaling vs.  $V_g/V$  is valid, it is obvious that the fragility parameter  $m_T$  [see its definition in Chap. 1 (1.26)], calculated at the glass transition point, is a material constant independent of pressure. Let us analyze how this feature affects the other fragilities  $m_V$  and  $m_P$ . In order to do that, we find relationships between the quantities at the point  $(P, T_g(P), V(P, T_g(P)))$ . From the definition of the isothermal fragility, one can derive, by exploiting the rule of the implicit partial derivative, the relationship between  $m_T$  and  $m_V$ :

$$\begin{aligned} m_T &= \left( \frac{\partial \log_{10}(\tau)}{\partial (V_g/V)} \right) \Big|_{T=T_g} = - \left( \frac{V^2}{V_g} \frac{\partial \log_{10}(\tau)}{\partial V} \right) \Big|_{T=T_g} \\ &= \left[ \left( -\frac{V^2}{V_g} \right) \cdot \left( - \left( \frac{\partial \log_{10}(\tau)}{\partial (T_g/T)} \right) \Big|_{T=T_g} / \left( \frac{\partial V}{\partial (T_g/T)} \right) \Big|_{T=T_g} \right) \right] \Big|_{V=V_g} \\ &= - \frac{m_V}{T_g \alpha_{\tau}(T_g)}. \end{aligned} \quad (2.41)$$

As shown in (2.17) the inverse negative product of the glass transition temperature  $T_g$  and the isochronic thermal volume expansivity calculated at the same temperature  $T = T_g$  is equal to the scaling exponent  $\gamma$ . Consequently, we get a new interesting relation between the isothermal and isochoric fragilities:

$$m_T = \gamma m_V \quad (2.42)$$

which means that the isochoric fragility  $m_V$  has to be pressure independent in order for  $\gamma$  to remain constant in accordance with the requirements from the thermodynamic scaling. Referring to calculations from (2.6), one can obtain, even independent of the last two equations, how the parameters  $m_T$  and  $m_P$  are mutual related:

$$\begin{aligned} m_P &= - \left( \frac{\partial \log_{10}(\tau)}{\partial V} \right) \Big|_{T|V=V_g} \left( \frac{\partial V}{\partial(T_g/T)} \right) \Big|_{\tau|T=T_g} + \left( \frac{\partial \log_{10}(\tau)}{\partial V} \right) \Big|_{T|V=V_g} \left( \frac{\partial V}{\partial(T_g/T)} \right) \Big|_{P|T=T_g} \\ &= \left( -\frac{T^2}{T_g} \right) \cdot \left( -\frac{V_g}{V^2} \right) \\ &\quad \cdot \left( - \left( \frac{\partial \log_{10}(\tau)}{\partial(V_g/V)} \right)_T \left( \frac{\partial V}{\partial T} \right)_\tau + \left( \frac{\partial \log_{10}(\tau)}{\partial(V_g/V)} \right)_T \left( \frac{\partial V}{\partial T} \right)_P \right) \Big|_{T=T_g, V=V_g}. \end{aligned} \quad (2.43)$$

Consequently, the ratio of isobaric and isothermal fragilities can be expressed as follows:

$$\frac{m_P}{m_T} = -T_g \alpha_\tau(T_g) + T_g \alpha_P(T_g). \quad (2.44)$$

It can be easily seen that the above equation is equivalent to (2.7) due to the relation derived in (2.41). Moreover, taking into account (2.17), the ratio from (2.44) leads to the following relation that is satisfied once the thermodynamic scaling is valid:

$$m_P = \frac{m_T}{\gamma} (1 + \gamma T_g \alpha_P(T_g)) \quad (2.45)$$

which is equivalent to (2.10) due to (2.42). The detailed analysis above shows that the experimentally known pressure dependence of the isobaric fragility results only from the pressure dependence of the product  $T_g \alpha_P(T_g)$  while the thermodynamic scaling is obeyed.



The above consequences of the thermodynamic scaling show that the Spencer–Boyer rule [36, 37],  $T_g \alpha_P(T_g) \approx \text{const}$ , and the following set of empirical correlations suggested by Casalini and Roland [38], namely,

1. The linear correlation between the isobaric and isochoric fragilities

$$m_P = m_0 + a m_V. \quad (2.46)$$

2. The inverse linear correlation between the scaling exponent  $\gamma$  and the isochoric fragility

$$\gamma = \gamma_0 + b m_V^{-1}, \quad (2.47)$$

are generally limited to ambient pressure conditions. The constant parameters of linear regressions in terms of (2.46) and (2.47), that is,  $m_0 = 37 \pm 3$ ,  $a = 0.84 \pm 0.05$ ,  $\gamma_0 = -1.042$ , and  $b = 217$ , determined at atmospheric pressure [38, 39] for several glass-forming liquids could be generalized for elevated pressures only in the case of (2.47). This is obvious because the isochoric fragility  $m_V$  has been argued to be pressure independent once the thermodynamic scaling is valid. However, the pressure dependences  $m_0(P)$  and  $a(P)$  are expected not to be constant [40, 41], reflecting the experimentally observed changes in the isobaric fragility,  $m_P$ , with increasing pressure, that is typically a decreasing function of pressure in vdW liquids and polymers.

It is worth noting that (2.46) is not the only correlation found at ambient pressure that is broken when liquids are compressed. The next example is a rather rough correlation between the isobaric fragility  $m_P$  and the stretching exponent  $\beta_{\text{KWW}}$  of the Kohlrausch–Williams–Watts function [42],  $m_P = 250 \pm 30 - 320\beta_{\text{KWW}}$ , which has been suggested by Böhmer et al. [43] at atmospheric conditions. This relation cannot give proper values of  $m_P$  at elevated pressures, since Ngai et al. [44] have recently shown, for several glass formers, which the parameter  $\beta_{\text{KWW}}$ , that characterizes the breadth and asymmetry of the structural relaxation peak, does not change with pressure (Chap. 1).

### 2.1.5 Doubts About the Thermodynamic Scaling Universality

Unfortunately, the above-presented appealing idea of the thermodynamic scaling cannot be treated as a universal method for the description of the structural relaxation in viscous systems.

Using high pressure measurements, it has been shown that the thermodynamic scaling vs.  $T$  cannot be valid for strongly hydrogen bonded systems such as DPG

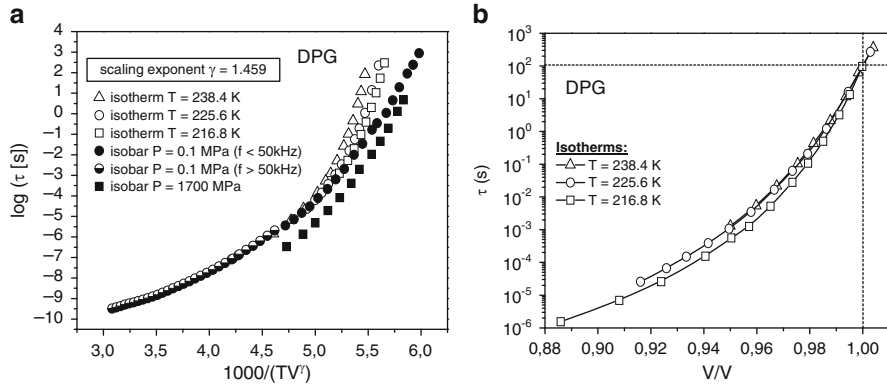


**Fig. 2.6** No scaling of structural relaxation times for DPG: (a) Plot of  $\alpha$ -relaxation times vs. the quantity  $\Gamma = T^{-1}V^{-\gamma}$ ; (b) the scaling plot of isothermal  $\alpha$ -relaxation times vs.  $V_g/V$ .

[40, 41] (see Fig. 2.6a) and water (from viscosity data) [45]. Similar results can be observed, although not so clearly, for glycerol for which many points shown in the master plot [46] diverge from one curve originally treated as a master curve according to (2.32). Later on, some of us have established by analyzing data for DPG [28] (see Fig. 2.6b) that the invalidity of the scaling vs.  $V_g/V$  can also be a common feature of molecular dynamics of materials forming H-bonded networks. The experiment-based analysis allows us to surmise that the expectation of the pressure independence of the scaling exponent  $\gamma$  can even be at variance with intrinsic properties of these materials, where the molecular structures especially vary with changing  $P$ ,  $V$ , and  $T$ , because the thermodynamic conditions strongly affect the degree of H bonds (see also Chap. 5 on the pressure effects on polymer blends). This is also a credible reason for excluding H-bonded systems from the correlations given by (2.46) and (2.47). The invalidity of the thermodynamic scaling for associated liquids has been recently supported by molecular dynamics simulations performed by Dyre's group [14, 15, 47]. By using commonly known force fields for water (such as SPC/E and TIP5P), they have demonstrated that strongly H-bonded liquids do not obey a strong correlation between equilibrium fluctuations of the configurational parts of pressure and energy. This is in contrast to the LJ systems and other simple vdW liquids, such as OTP and toluene, that fulfill the correlation in the high viscous region where cooperative and local dynamic processes play a main role.

It is worth noting that the mentioned simulations yield an elegant way of determining the scaling exponent  $\gamma$  as a function of the exponent of the repulsive term of the LJ potential, which has also been confirmed by Coslovich and Roland [16]. However, results obtained by Bailey et al. [14] for OTP demand to rethink about relations between thermodynamics and dynamics suggested by the thermodynamic scaling. The mentioned simulations lead to a surprising value of the scaling exponent for OTP, that is  $\gamma_{MD} \approx 8.0$ , which is about 2 times larger than

that suggested from inelastic neutron scattering [5] and later established from the thermodynamic scaling of different relaxation and viscosity data of some glass-forming liquids (KDE, PDE, OTP, BMMPC, and BMPC) as  $\gamma \approx 4.0$  [6, 8]. It is interesting that the calculations based on simulations, and some equations of state derived for the low compressibility region, which have common theoretical grounds outlined below, yield similar results.

The computational idea originates from the commonly known expression for instantaneous pressure,  $p = NkT/V + W/V$ , where  $N$  is the number of species of momenta  $\mathbf{p}_1, \dots, \mathbf{p}_N$  and positions  $\mathbf{r}_1, \dots, \mathbf{r}_N$  in volume  $V$ ;  $k$  is the Boltzmann constant;  $T = T(\mathbf{p}_1, \dots, \mathbf{p}_N)$  is treated as “kinetic temperature” proportional to the kinetic energy per particle; and  $W = W(\mathbf{r}_1, \dots, \mathbf{r}_N)$  is the virial which yields a configurational contribution to pressure. In general, the virial can be calculated for a translationally invariant function of the potential energy  $U = U(\mathbf{r}_1, \dots, \mathbf{r}_N)$  by using the formula  $W = -(1/3) \sum_i \mathbf{r}_i \cdot \nabla_i U$ , as it is usually done in computer

simulations [48]. Within the framework of the thermodynamic perturbation theory, a configurational contribution to pressure  $P_r = \langle W \rangle / V_0$  can be expressed in analogy by means of the average perturbed virial with the canonical distribution function of a reference state with a volume of  $V_0$ . However, in the case of simulations, we may take into account only the virial and potential energy values which are averages,  $\langle W \rangle$  and  $\langle U \rangle$ , respectively, in an appropriate thermodynamic ensemble practically evaluated as some time-averages. The tested correlation has been expected to relate linearly just those averages.

If, on the contrary, one assumes that a repulsive part of the intermolecular potential is a homogeneous function with the homogeneity exponent  $m_r$ , as in (2.2), then one can find an equation of state derived from such a molecular potential, which herein is presented for a specific volume  $V$ . The Euler theorem on homogeneous functions applied to the potential  $U$  reveals a useful property of the intermolecular potential,

$$U(s\mathbf{r}_1, \dots, s\mathbf{r}_N) = s^{-m_r} U(\mathbf{r}_1, \dots, \mathbf{r}_N). \quad (2.48)$$

If a similarity  $\mathbf{r} \rightarrow s\mathbf{r}$  is additionally considered, which scale,  $s = (V/V_0)^{1/3} = (\rho_0/\rho)^{1/3}$ , can be determined by using a specific volume  $V$  or density  $\rho$  (where  $V_0$  and  $\rho_0$  are, respectively, specific volume and density at a reference state), one can explain that the volume factor of the scaling quantity  $\Gamma$  from (2.1) is expressed by  $V^{m_r/3}$  as well as one can propose a state equation for the elevated pressure region [49],  $P = (RT/Mv) + (V_0/V)^{m_r/3} P_r$ , where  $R$  is the gas constant,  $M$  is the molar mass of substance, and  $P_r$  denotes herein a configurational contribution to pressure given by species of total mass equal to a unit mass of substance, which interact with each other by repulsive forces. However, the state equation is rather of low use for fitting  $PVT$  experimental data due to an undefined density–temperature dependence of the parameter  $P_r$  in the case of most real materials. Therefore, some

generalized form of the state equation has been introduced by Bardik and Shakun [50], which is presented here for a specific volume  $V$ :

$$P = \frac{RT}{MV} \left[ 1 + \varphi \left( \frac{1}{kT} \left( \frac{V_0}{V} \right)^{m_r/3} \right) \right]. \quad (2.49)$$

The unknown form of the  $\varphi$ -function can be derived by expanding in a series about a reference point with specific volume  $V_0$ , which is assumed to be characterized by a low isothermal compressibility. Then, taking into account only terms of the series up to the first order, the following expression for pressure can be obtained:

$$P = \frac{RT}{MV} \times \left[ 1 + \varphi \left( \frac{1}{kT} \left( \frac{V_0}{V} \right)^{m_r/3} \right) \right] \Big|_{V=V_0} + \frac{1}{kT} \varphi' \left( \frac{1}{kT} \left( \frac{V_0}{V} \right)^{m_r/3} \right) \Big|_{V=V_0} \left( \left( \frac{V_0}{V} \right)^{m_r/3} - 1 \right) \right] \quad (2.50)$$

Remembering that  $m_r = 3\gamma$  in (2.2) and making additional assumptions that the configurational pressure in the reference state is given by

$$P_0 = \phi \left( \frac{1}{kT} \left( \frac{V_0}{V} \right)^{m_r/3} \right) \Big|_{V=V_0} \frac{RT}{MV},$$

and the first-order coefficient is only temperature dependent,

$$B(T) = \phi' \left( \frac{1}{kT} \left( \frac{V_0}{V} \right)^{m_r/3} \right) \Big|_{v=v_0} \frac{R}{MVk},$$

one can rewrite (2.50) as follows:

$$P = \frac{RT}{MV} + P_0 + B(T) \left[ \left( \frac{V_0}{V} \right)^\gamma - 1 \right], \quad (2.51)$$

which is the equation-of-state convenient to test the hypothesis about a single scaling parameter  $\gamma$  by using isothermal  $PVT$  data [52, 53]. Recently, deriving (2.51) from the definition of the configurational isothermal bulk modulus  $B_T^{conf} \equiv -V \frac{\partial P^{conf}}{\partial V} \Big|_T = -\gamma \frac{\partial P^{conf}}{\partial \ln V^\gamma} \Big|_T$ , where the configurational pressure  $P^{conf} \equiv P - \frac{RT}{MV}$ , a physical meaning of the temperature dependent parameter  $B(T)$  has been found [53] by expressing it as  $B(T) = B_T^{conf}(P_0)/\gamma$ . It is worth mentioning that earlier attempts [23, 32] to discuss an equation of state in the context of

thermodynamic scaling did not involve successfully any explicit form of the term coming from a contribution of repulsive interactions. As theoretical investigations [14–16, 23] lead to the conclusion that an inverse power law approximation of intermolecular potential is appropriate to describe dynamic properties of dense, highly viscous liquids, it is well-founded to apply the equation of state [(2.51)], derived for the low compressibility region, in studying the thermodynamic behavior of such materials.

Grzybowski et al. [52, 53] have tested fits of isothermal volumetric data to (2.51) for some representatives of vdW liquids, weakly H-bonded liquids, and polymers; phenylphthalein-dimethylether (PDE), OTP, propylene carbonate (PC), meta-fluor-oaniline (m-FA), and 1,2-polybutadiene (1,2-PB). As it can be seen, for example, for OTP in Fig. 2.7, the accuracy of the fitting procedure to (2.51) is high due to prior calculation of the parameter  $P_0$  for each isotherm at a point  $(V_0, P(V_0))$  chosen separately for each isotherm and characterized by the locally lowest experimentally achieved isothermal compressibility. The scaling exponents,  $\gamma_{es}$ , found from the equation of state, which are presented in Table 2.1, are surprisingly at least two times larger than those determined from the standard scaling procedure based on (2.1). However, it is especially interesting to compare for OTP the scaling exponents  $\gamma_{es} \approx 10.0$  and  $\gamma_{MD} \approx 8.0$ , with the value  $\gamma$  obtained from the standard scaling procedure. The result that both  $\gamma_{es}$  and  $\gamma_{MD}$  are comparable and considerably larger than  $\gamma \approx 4.0$  is striking, because both the equation-of-state and calculations based on MD simulations come from the common theoretical grounds following from the virial theorem and the potential energy mainly governed by repulsive interactions in the case of highly viscous liquids. Some doubts about the thermodynamic scaling idea as a

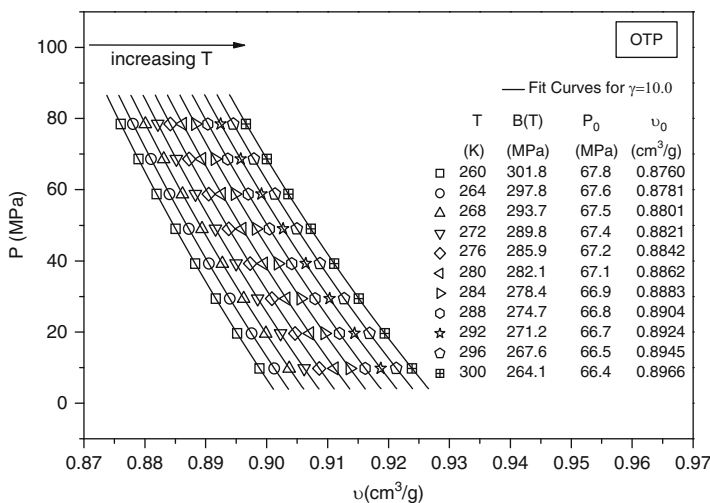


**Fig. 2.7** Plot of isothermal  $PVT$  data for ortho-terphenyl, which is generated by using the Tait equation with its parameters proposed in [8] and retaining the original measurement range reported in [51]. Solid lines denote fits of the data to the equation of state given by (2.51) first presented in Fig. 2 in [52]

**Table 2.1** Comparison of the values of scaling exponent  $\gamma$  earlier established from relaxation data by using (2.1) with those evaluated herein from volumetric data by fitting to the equation of state given by (2.51)

	$\gamma_r$ [ $\gamma$ found from (2.1)]	$\gamma_{es}$ [ $\gamma$ found from (2.51)]	$\gamma_{es}/\gamma_r$
PDE	4.5 <sup>a</sup>	9.2 $\pm$ 0.2	2.04
OTP	4.0 <sup>b</sup>	10.0 $\pm$ 0.1	2.50
PC	3.7 <sup>c</sup>	9.4 $\pm$ 0.1	2.54
m-FA	2.7 <sup>d</sup>	7.2 $\pm$ 0.1	2.67
1,2-PB	1.9 <sup>a</sup>	9.4 $\pm$ 0.1	4.95

<sup>a</sup>From [7]

<sup>b</sup>From [6]

<sup>c</sup>From [10]

<sup>d</sup>From [46]

linkage between dynamic and thermodynamic properties of supercooled liquids arise from such a significant discrepancy between the scaling exponents  $\gamma_{es}$  and  $\gamma$ . Moreover, the finding strongly suggests that even if the thermodynamic scaling were valid at least for vdW and polymer systems in the sense considered so far, its genuine bases require to be reanalyzed. Finally, it is worth mentioning that in contrast to MD simulations, where attractive forces have to be involved, the last term describing the configurational pressure in the equation of state (2.51) is an approximation based mainly on the repulsive interactions contribution, where the attractive interactions can be considered as some nearly constant background. However, we would like to emphasize that such an approximation made for highly viscous systems cannot downgrade the conclusions drawn on that basis. It is related to some theoretical analyses first performed by Weeks et al. [54] at the beginning of the 1970s. According to them, the thermodynamic and structural properties of the LJ fluid are dominated by the repulsive part at high temperatures for all densities as well as at low temperatures for high densities.

Very recently, within the framework of the temperature-volume Avramov model described in Sect. 2.1.3, a meaningful progress in explaining the discrepancies between the found values of the exponents  $\gamma$  and  $\gamma_{es}$  has been made [55, 56]. Making a reasonable assumption that the maximal energy barrier in (2.24) can be scaled in terms of specific volume or density with some scaling exponent  $\gamma_E$ , i.e.,  $E_{\max}(V) = A_E(V_r/V)^{\gamma_E}$ , where  $A_E$  is some material constant that has energy units, the temperature-volume Avramov model has been adjusted to better describe dynamics of real glass-forming materials in the vicinity of the glass transition. Applying this assumption to (2.24), we find the following modified equation,

$$\begin{aligned} \log_{10}[\tau(\Gamma)] &= \log_{10}(\tau_{\infty}) + (A\Gamma)^D, \quad \Gamma = T^{-1}V^{-\gamma}, \\ A &= [\in \log_{10}(e)]^{1/D}/\Gamma_r, \quad \Gamma_r = T_r^{-1}V_r^{-\gamma}, \quad \in = A_E/\sigma_r \end{aligned} \quad (2.52)$$

Since the value of the scaling exponent  $\gamma_E$  has turned out to be in very good agreement with that of  $\gamma_{es}$  found by fitting PVT data to the equation of state [(2.51)] for each tested representative of vdW liquids [55] and one ionic liquid

[56] near the glass transition, the scaling exponent  $\gamma$  in (2.52) can be related to the Grüneisen constant  $\gamma_G$  and the exponent  $\gamma_{es}$  as follows

$$\gamma = \gamma_G + \gamma_{es}/D \quad (2.53)$$

The relation is expected to have an important impact on our understanding of linkages between thermodynamic and dynamic properties of materials near the glass transition as well as intermolecular interactions responsible for the thermodynamic scaling, but it requires further investigations and tests for various materials.

## 2.2 The Role of Monomer Volume and Local Packing on the Glass-Transition Dynamics

The thermodynamic scaling has advantages as well as some problems as discussed above. In addition, the proposed scaling lacks a predictive power; i.e., given a molecular structure it cannot make suggestions on the thermodynamic parameter that mostly affects the dynamics. Some of us suggested on a different way [57] of analyzing the dynamic quantity  $Q_V/Q_P$  that provides a quantitative measure of the relative importance of  $\rho$  and  $T$  in the dynamics of the  $\alpha$ -process. We demonstrate – without invoking any scaling – that the repeat unit volume and local packing play a key role in controlling this ratio and thus the dynamics of glass formers near  $T_g$ . We start by collecting literature  $Q_V/Q_P$  values from the different glass-forming systems at  $P = 0.1$  MPa and at  $T_g$  (defined at  $\tau = 1$  s) (obtained mainly by dielectric spectroscopy and light scattering) in Table 2.2

Apart from the dynamic ratio,  $Q_V/Q_P$ , we discuss a well-known property of amorphous systems and glass-forming liquids, namely, the presence of a degree of packing regularity reflected by the broad peaks in the wide-angle X-ray or neutron scattering curves [58–60]. For polymers in particular, the peak at higher values of the wave vector  $q$ , with an equivalent Bragg spacing of about 0.5 nm, corresponds to the vdW (VDW) contacts of atoms and is known as the vdW peak. The peak at lower  $q$ , known as the low van der Waals (LvdW) peak, reflects largely the intermolecular correlations of polymeric backbones. There are some exceptions to this; in bisphenol A polycarbonate (BPA-PC), the first (shallow) peak at  $q^* \sim 6 \text{ nm}^{-1}$  is caused mainly by the correlation between the carbonate groups, i.e., it is of intramolecular origin. On the contrary, for glass-forming liquids, the origin of the diffraction peaks and their  $q^*(T)$  is not well understood.

In Table 2.2, the position of the LVDW peak for various glass-forming systems is reported and allows the correlation of this “static” quantity (the reported  $q^*$  values are in most cases measured in the vicinity of  $T_g$ ) with the dynamic ratio  $Q_V/Q_P$ , obtained at  $T_g$  ( $P = 0.1$  MPa,  $\tau = 1$  s). This correlation is by no means perfect; however, in extreme cases, it allows for some conclusions. For example, in glass-formers with  $q^* < 5 \text{ nm}^{-1}$ , the ratio  $Q_V/Q_P$  is below 0.6. Similarly, in glass formers with  $q^* > 15 \text{ nm}^{-1}$ , the ratio  $Q_V/Q_P$  is higher than 0.6. The meaning of these correlations is that in main-chain flexible polymers (high  $q^*$ ), temperature

**Table 2.2** Sample code and name, glass temperature, repeat unit volume ( $V_m$ ), characteristic wave vector ( $q^*$ ) of the first intense peak of the static structure factor, and ratio of the constant volume activation energy ( $Q_V$ ) to the enthalpy of activation ( $Q_P$ )

Code	Sample	$T_g$ (K)	$V_m$ (nm <sup>3</sup> )	$q^*$ (nm <sup>-1</sup> )	$Q_V/Q_P$ [ $P = 1\text{ atm}$ , $T_g$ ( $\tau = 1\text{ s}$ )]
A	Poly(methyl- <i>p</i> -totyl siloxane) (PMpTS)	249.9	0.212	6.3	0.59
		261			0.55
B	Bisphenol A polycarbonate (BPAPC)	414	0.364	12.3	0.44
C	Poly(vinyl methyl ether) (PVME)	245.5	0.091	9.7	0.7
D	Poly(4-vinyl phenol) (PVPh)	443	–	14.1	~0.77
E	Polystyrene (PS)	373	0.169	8	0.64
F	Poly(2-vinyl pyridine) (P2VP)	367	0.185	7.8	0.7
G	1,4-Polybutadiene (PB)	263	0.093	15	0.76 <sup>a</sup>
H	Poly(methyl acrylate) (PMA)	276	0.119	9.4	0.78 <sup>b</sup>
I	Polyethylene (PE)	200	0.044	13.7	0.71–0.76
		225			0.81–0.85
J	1,2-Polybutadiene (PB)	253	0.094	10	0.7
K	Poly(vinyl ethyl ether) (PVEE)	240.6	0.113	8.2	0.81
L	Poly(propylene glycol) (PPG)	202.5	0.068	12.4	0.66
M	1,4-Polyisoprene (PI)	203	0.118	14	0.78
N	Polyvinylacetate (PVAc)	311	0.121	9.9	0.6
O	Poly(methyl phenyl siloxane) (PMPS)	245.7	0.171	7.2	0.46
P	Poly( <i>t</i> -butyl methacrylate) (PrBMA)	334	0.230	7.1	0.56
Q	Poly( <i>n</i> -ethyl methacrylate) (PnEMA)	326.7	0.170	5.6	0.55
R	<i>o</i> -terphenyl (OTP)	243.5	0.342	9.0	0.55
S	salol	220	0.282	8.0	0.43 ± 0.2
T	1,1'-bis( <i>p</i> -methoxy phenyl) cyclohexane (BMPC)	241	0.34	7.8	0.38
U	1,1'-di(4-methoxy-5-methyl phenyl) cyclohexane (BMMPC)	261	0.368	7.6	0.41
V	Phenolphthalein dimethylether (PDE)	249	0.419	–	0.52
W	Cresolphthalein dimethylether (KDE)	313	0.551	–	0.49
X	Poly[(phenyl glycidylether)- <i>co</i> -formaldehyde] (PPGE)	258	0.243	–	0.62
Y	Poly[( <i>o</i> -cresol glycidylether)- <i>co</i> -formaldehyde] (PCGE)	285	0.23	–	0.65
Z	Diglycidylether of bisphenol A (DGEBA)	335	0.4	–	0.6
1	Polyvinyl chloride (PVC)	353	0.076	–	0.8
2	Polyoxybutylene (POB)	199	0.116	–	0.75

<sup>a</sup>At  $T = T_g + 100\text{ K}$ <sup>b</sup>At  $T = T_g + 31\text{ K}$ 

through the energy barriers ( $k_B T$ ) provides the main means of affecting the dynamics. Instead, in polymers with bulky side-groups (low  $q^*$ ), volume effects gain importance and the dynamics are controlled by both  $\rho$  and  $T$ . Nonetheless, this correlation is not always exact. For example, BPA-PC with a low  $Q_V/Q_P$  value (~0.44) [61] has a high  $q^*$  value. This implies that parameters other than the mere interchain distance also play a role.

The broad correlation improves considerably if both the lateral distance and the distance along the backbone per repeat unit are taken into account. This is shown in



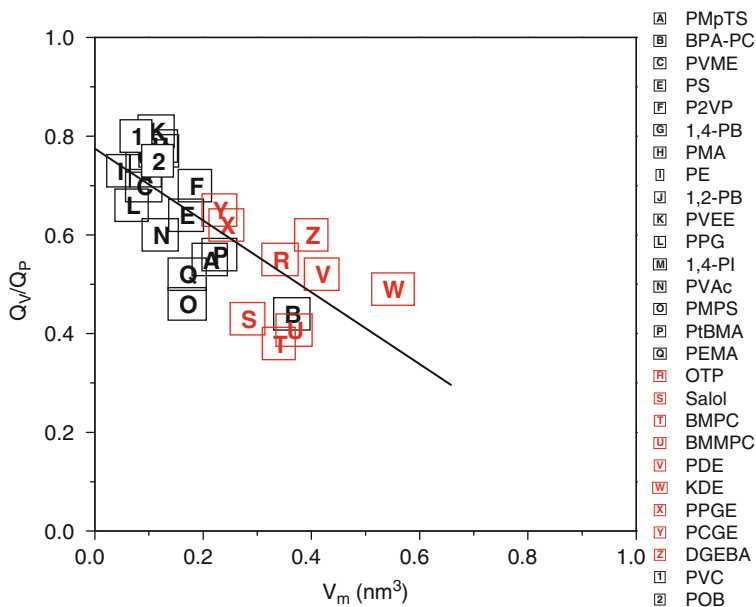


**Fig. 2.8** Ratio of the constant volume activation energy ( $Q_V$ ) to the enthalpy of activation ( $Q_P$ ) plotted as a function of the repeat unit volume (polymers) or the molecular volume (glass-forming liquids). The results from the glass-forming liquids are presented in color. Notice the lower values of the dynamic ratio for the glass-forming liquids that result from the larger size of these molecules necessary to avoid crystallization. The line is the result of a linear fit to all data points (from [57])

Fig. 2.8 where the dynamic ratio is plotted as a function of the repeat unit volume ( $V_m = M/\rho N_A$ , where  $M$  is the molecular weight of the repeat unit).

This dependence suggests that the reason for the very low  $Q_V/Q_P$  values of some glass-forming liquids and some polymers (BPA-PC) is their large repeat unit volume. In the same figure, additional data from other glass-forming liquids are also included. Notice that the reason for the higher  $Q_V/Q_P$  values of poly[(phenyl glycidylether)-*co*-formaldehyde] (PPGE) and poly[(*o*-cresol glycidylether)-*co*-formaldehyde] (PCGE) compared to those of the other glass-forming liquids is the smaller volume of their repeat unit. Similarly, the low values of the activation ratio in the case of glass-forming liquids result from their larger molecular volume [57]. Large monomer volumes and irregular shapes are required as they inhibit crystallization. We mention here that the good correlation of the dynamics with the static properties such as packing and repeat unit volume can be extended to include other variables that control the dynamics, such as the Kuhn length and the packing length [62].

Thus the repeat unit volume and local packing play a key role in controlling the value of this ratio at  $T_g$ , and the dynamics associated with the glass temperature. In particular, for *flexible* main-chain polymers, temperature, through the presence of energy barriers opposing molecular motions, is the main parameter affecting the

dynamics, whereas in polymers with *bulky side-groups* or in glass-forming liquids with large molar volumes, volume effects gain importance. These ideas are by no means new. A similar conclusion was reached by a recent theory of glass formation by Dudowicz, Freed, and Douglas [63] that emphasizes the importance of repeat unit volume, and backbone and side-group rigidity. In addition, Ngai and Roland [64] showed that the degree of intermolecular cooperativity of motions and the fragility reflect these same properties, namely, backbone flexibility and the presence of bulky side-groups. What is new, however, in this approach is that it provides a quantitative account of the value of the dynamic ratio, and thus of the parameters that most affect the dynamics, in relation to the molecular volume and packing.

The monomer volume approach that emphasizes the packing properties is different from the thermodynamic scaling because it includes the attractive forces that control the packing and the thermodynamic state. It also suggests that a general theory of liquid dynamics, applicable to all  $\rho$  and  $T$  and for all glass formers should, take into account both the repulsive and attractive parts of the potential function.

The proposed correlation between the local packing and the value of the dynamic ratio also has consequences with respect to the issue of dynamic heterogeneity in polymer blends and copolymers [65]. The appropriate choice of monomers in these could result in drastically different  $T$  and  $P$  dependencies for the two components, with consequences on their dynamic and possibly their thermodynamic miscibility (see Chap. 5).

## References

1. Angell CA (1995) *Science* 67:1924
2. Stillinger FH (1995) *Science* 267:1935
3. Ferry JD (1980) *Viscoelastic properties of polymers*, 3rd edn. Wiley, New York
4. Cohen MH, Grest GS (1979) *Phys Rev B* 20:1077
5. Tölle A (2001) *Rep Prog Phys* 64:1473
6. Dreyfus C, Aouadi A, Gapinski J, Matos-Lopes M, Steffen W, Patkowski A, Pick RM (2003) *Phys Rev E* 68:011204
7. Casalini R, Roland CM (2004) *Phys Rev E* 69:062501
8. Dreyfus C, Le Grand A, Gapinski J, Steffen W, Patkowski A (2004) *Eur Phys J B* 42:309
9. Alba-Simionesco C, Cailliaux A, Alegria A, Tarjus G (2004) *Europhys Lett* 68:58
10. Pawlus S, Casalini R, Roland CM, Paluch M, Rzoska SJ, Ziolo J (2004) *Phys Rev E* 70:061501
11. Roland CM, Hensel-Bielowka S, Paluch M, Casalini R (2005) *Rep Prog Phys* 68:1405
12. Hoover WG, Ross M (1971) *Contemp Phys* 12:339
13. Casalini R, Roland CM (2007) *J Non-Cryst Solids* 353:3936
14. Bailey NP, Pedersen UR, Gnan N, Schröder TB, Dyre JC (2008) *J Chem Phys* 129:184507
15. Bailey NP, Pedersen UR, Gnan N, Schröder TB, Dyre JC (2008) *J Chem Phys* 129:184508
16. Coslovich D, Roland CM (2009) *J Chem Phys* 130:014508
17. Williams G (1964) *Trans Faraday Soc* 60:1556
18. Naoki M, Endou H, Matsumoto K (1987) *J Phys Chem* 91:4169
19. Ferrer ML, Lawrence C, Demirjian BG, Kivelson D, Alba-Simionesco C, Tarjus G (1998) *J Chem Phys* 109:8010
20. Casalini R, Roland CM (2005) *Phys Rev B* 71:014210

21. Niss K, Alba-Simionesco C (2006) *Phys Rev B* 74:024205
22. Niss K, Dalle-Ferrier C, Tarjus G, Alba-Simionesco C (2007) *J Phys Condens Matter* 19:076102
23. Alba-Simionesco C, Tarjus G (2006) *J Non-Cryst Solids* 352:4888
24. Mpoukouvalas K, Floudas G, Williams G (2009) *Macromolecules* 42:4690
25. Boyer RF, Spencer RS (1944) *J Appl Phys* 15:398
26. Van Krevelen DW (1990) *Properties of polymers*. Elsevier, New York
27. Casalini R, Roland CM (2004) *Colloid Polym Sci* 283:107
28. Paluch M, Grzybowska K, Grzybowski A (2007) *J Phys Condens Matter* 19:205117
29. Corezzi S, Capaccioli S, Casalini R, Fioretto D, Paluch M, Rolla PA (2000) *Chem Phys Lett* 320:113
30. Casalini R, Mohanty U, Roland CM (2006) *J Chem Phys* 125:014505
31. Hartwig G (1994) *Polymer properties at room and cryogenic temperatures*, Chap. 4. Plenum, New York
32. Roland CM, Feldman JL, Casalini R (2006) *J Non-Cryst Solids* 352:4895
33. Grüneisen E (1912) *Ann Phys (Leipzig)* 39:257
34. Moelwyn-Hughes EA (1951) *J Phys Coll Chem* 55:1246
35. Roland CM (2008) In: Bhowmick AK (ed) *Current topics in elastomers research*, Chap. 24. CRC Press in Taylor & Francis Group, Boca Raton
36. Boyer RF, Spencer RS (1944) *J Appl Phys* 15:398
37. Van Krevelen DW (1990) *Properties of polymers*. Elsevier, New York
38. Casalini R, Roland CM (2005) *Phys Rev E* 72:031503
39. Casalini R, Capaccioli S, Roland CM (2006) *J Phys Chem B* 110:11491
40. Grzybowski A, Grzybowska K, Ziolo J, Paluch M (2006) *Phys Rev E* 74:041503
41. Grzybowski A, Grzybowska K, Ziolo J, Paluch M (2007) *Phys Rev E* 76:013502
42. Williams G, Watts DC (1970) *Trans Faraday Soc* 66:80
43. Böhmer R, Ngai KL, Angell CA, Plazek DJ (1993) *J Chem Phys* 99:4201
44. Ngai KL, Casalini R, Capaccioli S, Paluch M, Roland CM (2005) *J Phys Chem B* 109:17356
45. Roland CM, Bair S, Casalini R (2006) *J Chem Phys* 125:124508
46. Reiser A, Kasper G, Hunklinger S (2005) *Phys Rev B* 72:094204
47. Pedersen UR, Bailey NP, Schröder TB, Dyre JC (2008) *Phys Rev Lett* 100:015701
48. Allen MP, Tildesley DJ (1987) *Computer simulation of liquids*. Oxford University Press, Oxford
49. Bardic VY, Malomuzh NP, Sysoev VM (2005) *J Mol Liq* 120:27
50. Bardik VY, Shakun KS (2005) *Ukr J Phys* 50:404
51. Naoki M, Koeda S (1989) *J Phys Chem* 93:948
52. Grzybowski A, Paluch M, Grzybowska K (2009) *J Phys Chem B* 113:7419
53. Grzybowski A, Haracz S, Paluch M, Grzybowska K (2010) *J Phys Chem B* 114:11544
54. Weeks JD, Chandler D, Andersen HC (1971) *J Chem Phys* 54:5237
55. Grzybowski A, Paluch M, Grzybowska K, Haracz S (2010) *J Chem Phys* 133:161101
56. Paluch M, Haracz S, Grzybowski A, Mierzwa M, Pionteck J, Rivera-Calzada A, Leon C (2010) *J Phys Chem Lett* 1:987
57. Floudas G, Mpoukouvalas K, Papadopoulos P (2006) *J Chem Phys* 124:074905
58. Miller RL, Boyer R, Heijboer J (1984) *J Polym Sci Polym Phys Ed* 22:2021
59. Floudas G, Stepanek P (1998) *Macromolecules* 31:6951
60. Cailliaux A, Alba-Simionesco C, Frick B, Willner L, Goncharenko I (2003) *Phys Rev E* 67:010802
61. Mpoukouvalas K, Gomopoulos N, Floudas G, Herrmann C, Hanewald A, Best A (2006) *Polymer* 47:7170
62. Everaers R, Sukumaran SK, Grest GS, Svaneborg C, Sivasubramanian A, Kremer K (2004) *Science* 303:823
63. Dudowicz J, Freed K, Douglas JF (2005) *J Chem Phys* 123:111102
64. Ngai KL, Roland CM (1993) *Macromolecules* 26:6824
65. Floudas G, Fytas G, Reisinger T, Wegner G (1999) *J Chem Phys* 111:9129

Molecular Dynamics of Glass-Forming Systems  
Effects of Pressure

Floudas, G.; Paluch, M.; Grzybowski, A.; Ngai, K.

2011, XII, 176 p., Hardcover

ISBN: 978-3-642-04901-9